Physics Letters B 750 (2015) 448–452

Contents lists available at ScienceDirect

Physics Letters B

www.elsevier.com/locate/physletb

Lifetime measurements of the first 2^+ states in ^{104,106}Zr: Evolution of ground-state deformations

F. Browne [a,b,*], A.M. Bruce [a], T. Sumikama [c,b], I. Nishizuka [c], S. Nishimura [b], P. Doornenbal [b], G. Lorusso [b], P.-A. Söderström [b], H. Watanabe [d,b], R. Daido [e], Z. Patel [f,b], S. Rice [f,b], L. Sinclair [g,b], J. Wu [h,b], Z.Y. Xu [i,j], A. Yagi [e], H. Baba [b], N. Chiga [c,b], R. Carroll [f], F. Didierjean [k], Y. Fang [e], N. Fukuda [b], G. Gey [l,m,b], E. Ideguchi [e], N. Inabe [b], T. Isobe [b], D. Kameda [b], I. Kojouharov [n], N. Kurz [n], T. Kubo [b], S. Lalkovski [o], Z. Li [h], R. Lozeva [k], H. Nishibata [e], A. Odahara [e], Zs. Podolyák [f], P.H. Regan [f,p], O.J. Roberts [a], H. Sakurai [i,b], H. Schaffner [n], G.S. Simpson [l], H. Suzuki [b], H. Takeda [b], M. Tanaka [e], J. Taprogge [q,r,b], V. Werner [s,t], O. Wieland [u]

[a] School of Computing, Engineering and Mathematics, University of Brighton, Brighton, BN2 4GJ, United Kingdom
[b] RIKEN Nishina Center, 2-1 Hirosawa, Wako-shi, Saitama 351-0198, Japan
[c] Department of Physics, Tohoku University, Aoba, Sendai, Miyagi 980-8578, Japan
[d] IRCNPC, School of Physics and Nuclear Energy Engineering, Beihang University, Beijing 100191, China
[e] Department of Physics, Osaka University, Toyonaka, Osaka 560-0043, Japan
[f] Department of Physics, University of Surrey, Guildford GU2 7XH, United Kingdom
[g] Department of Physics, University of York, Heslington, York YO10 5DD, United Kingdom
[h] Department of Physics, Peking University, Beijing 100871, China
[i] Department of Physics, University of Tokyo, Hongo, Bunkyo-ku, Tokyo 113-0033, Japan
[j] Department of Physics, University of Hong Kong, Pokfulam Road, Hong Kong
[k] IPHC, CNRS/IN2P3, Université de Strasbourg, 67037 Strasbourg, France
[l] LPSC, Université Grenoble-Alpes, CNRS/IN2P3, F-38026 Grenoble Cedex, France
[m] ILL, 38042 Grenoble Cedex, France
[n] GSI Helmholtzzentrum für Schwerionenforschung GmbH, 64291 Darmstadt, Germany
[o] Department of Physics, University of Sofia, 1164 Sofia, Bulgaria
[p] National Physical Laboratory, Teddington, Middlesex, TW11 0LW, United Kingdom
[q] Departamento de Física Teórica, Universidad Autónoma de Madrid, E-28049 Madrid, Spain
[r] Instituto de Estructura de la Materia, CSIC, E-28006 Madrid, Spain
[s] A.W. Wright Nuclear Structure Laboratory, Yale University, New Haven, CT 06520, USA
[t] Institut für Kernphysik, Technische Universitäat Darmstadt, 64289 Darmstadt, Germany
[u] INFN Sezione di Milano, I-20133 Milano, Italy

ARTICLE INFO

Article history:
Received 24 July 2015
Received in revised form 9 September 2015
Accepted 16 September 2015
Available online 25 September 2015
Editor: V. Metag

ABSTRACT

The first fast-timing measurements from nuclides produced via the in-flight fission mechanism are reported. The lifetimes of the first 2^+ states in ^{104,106}Zr nuclei have been measured via β-delayed γ-ray timing of stopped radioactive isotope beams. An improved precision for the lifetime of the 2_1^+ state in ^{104}Zr was obtained, $\tau(2_1^+) = 2.90^{+25}_{-20}$ ns, as well as a first measurement of the 2_1^+ state in ^{106}Zr, $\tau(2_1^+) = 2.60^{+20}_{-15}$ ns, with corresponding reduced transition probabilities of $B(\mathrm{E2}; 2_1^+ \rightarrow 0_{g.s.}^+) = 0.39(2)$ $e^2\mathrm{b}^2$ and 0.31(1) $e^2\mathrm{b}^2$, respectively. Comparisons of the extracted ground-state deformations, $\beta_2 = 0.39(1)$ (^{104}Zr) and $\beta_2 = 0.36(1)$ (^{106}Zr) with model calculations indicate a persistence of prolate deformation. The data show that ^{104}Zr is the most deformed of the neutron-rich Zr isotopes measured so far.

* Corresponding author at: School of Computing, Engineering and Mathematics, University of Brighton, Brighton, BN2 4GJ, United Kingdom.
E-mail address: f.browne@brighton.ac.uk (F. Browne).

http://dx.doi.org/10.1016/j.physletb.2015.09.043

The shape of the atomic nucleus is one of its most fundamental properties. When the nuclear shells are filled to the "magic numbers" [1,2], the nucleonic distribution is spherical. In-between these major shell closures, the nuclear shape can stabilise to a non-spherical deformed configuration. The simplest of these is the quadrupole deformation, of which the two varieties are labelled as prolate (rugby ball) and oblate (discus) shapes. The quantification of these shapes in regions of the nuclear chart which display rapid shape changes as a function of nucleon number provides stringent tests to a variety of nuclear models. They also provide essential input for developing contemporary theoretical frameworks [3].

The zirconium isotopes ($Z = 40$) are located centrally with respect to the $1f_{7/2}$ ($Z = 28$) and $1g_{9/2}$ ($Z = 50$) major shell closures, making them an exemplary case study of mid-shell nuclei. The most abundant isotope of zirconium ($N = 50$) exhibits doubly magic behaviour due to the reinforcement of the *pf* proton shell closure at $Z = 40$ by the major $N = 50$ neutron shell closure [4,5]. A region of weak proton–neutron coupling follows [6,7] up to the nearly doubly-magic ^{96}Zr ($N = 56$) [8]. A rapid shape-phase transition (or shape coexistence) occurs across $N = 60$ [9–12], and from thereon a large degree of collectivity and static ground-state quadrupole deformation is manifest towards the middle of the $N = 50$–82 shell [12,13]. The onset of deformation has been ascribed to the proton–neutron interactions of the spin–orbit partner orbitals, $\pi g_{9/2}$ and $\nu g_{7/2}$ [14,15], and is reinforced in $N \geq 60$ nuclei by the increased occupancy of the high-j low-Ω $\nu h_{11/2}$ orbitals [16–19]. Laser spectroscopy measurements have shown this ground-state deformation to be strongly prolate for ^{101}Zr [20]. The axial symmetry of the $N > 60$ Zr isotopes is at odds with its higher-Z neighbours, which exhibit triaxiality [21–24], conversely lower-Z Sr isotopes exhibit a more severe transition to strongly deformed ground-state deformations [25]. The simplicity of their axially symmetric deformation could make the $N > 60$ Zr isotopes a good reference case for the global understanding of this wide mid-shell region. Although the number of active neutrons (or holes) is maximum at the mid-shell ($N = 66$), the observed increase of 2^+_1 energies suggests a decrease in deformation after $N = 64$ [13]. This has been discussed with respect to the possibility of an $N = 70$ sub-shell [26] with important implications for waiting points of the astrophysical *r*-process.

In this Letter, the first application of β-delayed γ-ray (β-γ) fast-timing measurements of radioactive isotope beams produced through the in-flight fission mechanism is used to measure the lifetimes of the 2^+_1 states in ^{104,106}Zr. The reduced transition probabilities, $B(\mathrm{E2}; 2^+_1 \rightarrow 0^+_{g.s.})$, an observable which measures the correlations between ground- and excited-states, are extracted and compared to theoretical values from projected shell model and algebraic model calculations. The quadrupole deformation of the ground-states are extracted from the $B(\mathrm{E2}; 2^+_1 \rightarrow 0^+_{g.s.})$ values and compared to a variety of nuclear mean-field calculations.

The experimental investigation of ^{104,106}Zr was carried out at the Radioactive Isotope Beam Factory (RIBF), operated by the RIKEN Nishina Center (RNC) and the Center for Nuclear Study, University of Tokyo. A ^{238}U^{86+} primary beam of average intensity 6.24×10^{10} particles/s was accelerated to an energy of 345 MeV/nucleon. The in-flight abrasion fission of the beam was induced by a 555 mg/cm^2 ^{9}Be production target situated at the entrance of the BigRIPS fragment separator [27]. Fission fragments were selected through the $B\rho$–ΔE–$B\rho$ method and identified using the TOF–$B\rho$–ΔE method [28]. The data were collected using two different settings of the BigRIPS and ZeroDegree spectrometers [27], centred on the β-decay parents of ^{104,106}Zr. A total of 6.2×10^5 ^{106}Y ions were transmitted in a wide-range and very neutron-rich setting, and 3.8×10^5 ^{104}Y ions in a setting with a focus on a less exotic region [29].

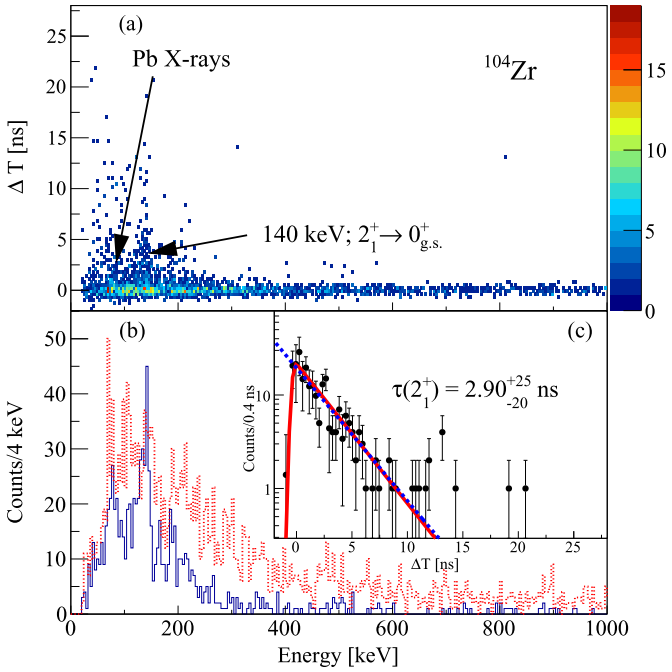

Fig. 1. (Colour online.) (a) Energy–time-difference matrix observed in coincidence with β-electrons detected within 1 s of an ^{104}Y implantation. (b) The γ-ray energy spectrum of the delayed (solid blue) and prompt (dashed red) components of the matrix. (c) Background subtracted time difference spectrum for the $2^+_1 \rightarrow 0^+_{g.s.}$ transition. (See text for details of the fits.)

The secondary beam was implanted into the WAS3ABi silicon array [30], which detected ion implantations and their subsequent β-decay electrons. For this experiment, WAS3ABi comprised 5 layers of double-sided silicon strip detectors placed 0.5 mm apart, each with 60 vertical and 40 horizontal strips. The width and depth of each strip were both 1 mm, giving a total active area of 60×40 mm^2. Candidate β decays had to be detected within the same implantation pixel as the preceding ion, and within approximately five times the β-decay half-life of the parent nuclide. For the purpose of precision timing of electrons for β–γ measurements, BC-148 plastic scintillators (β-plastics) of 2-mm thickness and area 65×45 mm^2 were installed upstream and downstream of WAS3ABi, these were each optically coupled to two photomultiplier tubes (PMT), with the arithmetic mean of the time signals used as the β^- detection time. The absolute efficiency of the β-plastics was ∼50%.

An array of 18 small $LaBr_3$(Ce) crystals was constructed for the measurement of level lifetimes in a low-yield and low-background environment [31]. This array, as well as the EURICA [32] HPGe array, surrounded WAS3ABi for the purpose of measuring isomeric and β-delayed γ rays. The nominal distance between the centre of WAS3ABi and the front of the $LaBr_3$(Ce) detectors was 24 cm and each cylindrical crystal had a diameter of 38.1 mm and a depth of 50.8 mm. At the energies of interest (150–170 keV) the absolute efficiency of the array was measured to be ∼4%, the energy resolution to be 10% and the time resolution FWHM = 825(25) ps. Energy–time matrices were constructed using the γ-ray energy measured in the $LaBr_3$(Ce) array, and the time-difference, ΔT, between the β^- and γ-ray detection. Figs. 1(a) and 2(a) show the matrices for ^{104}Zr and ^{106}Zr, respectively.

Figs. 1(b) and 2(b) show the prompt (red dashed line, $\Delta T < \pm 0.5$ ns) and delayed (solid blue line, $1.5 < \Delta T < 25$ ns) projections of γ-ray energy. Both show lead X-rays which are produced by γ-ray interactions with the passive anti-Compton lead shielding surrounding each $LaBr_3$(Ce) crystal. The delayed spectrum of

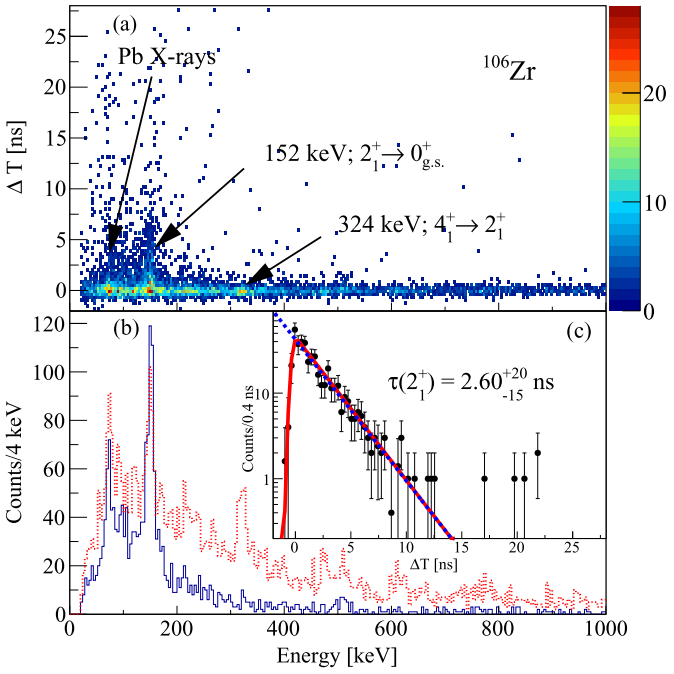

Fig. 2. (Colour online.) (a) Energy–time-difference matrix observed in coincidence with β^- detected within 0.3 s of an ^{106}Y implantation. (b) The γ-ray energy spectrum of the delayed (solid blue) and prompt (dashed red) components of the matrix. (c) Background subtracted time difference spectrum for the $2_1^+ \rightarrow 0^+_{g.s.}$ transition. (See text for details of the fits.)

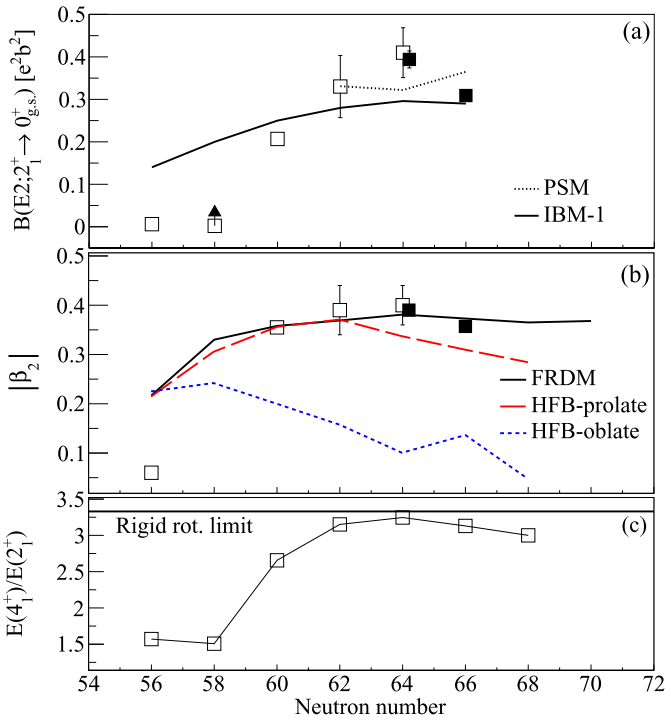

Fig. 3. (Colour online.) (a) Experimental $B(E2; 2_1^+ \rightarrow 0^+_{g.s.})$ values of even–even $^{96-106}$Zr isotopes, compared with the results of PSM [38] and IBM-1 [39] calculations. The arrow on the $N = 58$ point reflects the fact the data point is a limit. (b) Experimentally determined β_2 values for $^{100-106}$Zr, compared with the results of mean-field calculations. (c) The $E(4_1^+)/E(2_1^+)$ ratios for $^{96-108}$Zr. The open symbols are from Refs. [40–44,13] and closed symbols are from the current work.

Fig. 1(b) shows the 140-keV $2_1^+ \rightarrow 0^+_{g.s.}$ transition in ^{104}Zr. The delayed γ-ray energy spectrum of ^{106}Zr, Fig. 2(b) shows the 152 keV $2_1^+ \rightarrow 0^+_{g.s.}$ transition. It is noteworthy that in the prompt (red) spectrum of Fig. 2(b), the 324-keV $4_1^+ \rightarrow 2_1^+$ transition is clearly observed, implying strong feeding of the 2_1^+ state from the 4_1^+ state. Indeed, in both nuclei the efficiency-corrected intensities from the EURICA spectra indicate the feeding of the 2_1^+ levels is ∼50% from the 4_1^+ level and ∼20% each from two other, as yet, unassigned transitions with energies between 600–800 keV. The energy–time matrices of Figs. 1(a) and 2(a) indicate that there exist no measurable delayed structures from these transitions. Therefore, a systematic uncertainty of 50 ps has been included in the upper limit of the lifetime of the 2_1^+ state based on lifetimes of the 4_1^+ state estimated from Refs. [33–35].

Figs. 1(c) and 2(c) show the time-difference spectra for the $2_1^+ \rightarrow 0^+_{g.s.}$ transition of ^{104}Zr and ^{106}Zr, respectively. Lifetimes were extracted using two approaches. The first, fitted a single decay component to the delayed shoulder of the time-difference distribution between the limits of 2 and 10 ns, as shown by the dotted blue curve. Secondly, the solid red curve shows the result of using the convolution of the detector resolution and an exponential decay as the fit function. The resolution of the detector was assumed to be Gaussian shaped, with a width obtained from a fit to the $(5^-) \rightarrow (4^-)$ 159 keV transition in ^{102}Zr [36], which was observed to be prompt. We obtain consistent lifetimes with the two methods of $\tau(2_1^+) = 2.90^{+25}_{-20}$ ns and 2.60^{+20}_{-15} ns for ^{104}Zr and ^{106}Zr, respectively. The former is in agreement with the value in Ref. [37], 2.9(4) ns, but has a higher precision.

The $B(E2; 2_1^+ \rightarrow 0^+_{g.s.})$ values of Fig. 3(a) were obtained following the prescription of Ref. [45], yielding values of 0.39(2) e^2b^2 and 0.31(1) e^2b^2 for ^{104}Zr and ^{106}Zr, respectively. The β_2 values shown in Fig. 3(b) were derived from the $B(E2; 2_1^+ \rightarrow 0^+_{g.s.})$ values shown in Fig. 3(a), assuming a quadrupoloid shape and including terms to 3rd order [46]. For ^{104}Zr and ^{106}Zr, this procedure gives $\beta_2 = 0.39(1)$ and 0.36(1), respectively. The observation that the $E(4_1^+)/E(2_1^+)$ ratios, shown in Fig. 3(c), approach the limiting value of 3.33 for $N > 60$, provides evidence that the rigid-rotor model is a good approximation in which to interpret these nuclei. The new lifetime measurement shows that ^{104}Zr is the most deformed of the neutron-rich Zr isotopes.

Fig. 3(b) shows β_2 values calculated using the finite-range droplet model (FRDM) [47] (solid line), as well as prolate and oblate solutions of Hartree–Fock–Bogolyubov (HFB) calculations employing the Gogny-D1S interaction [48] (red and blue dashed lines, respectively). The FRDM predicts strong prolate minima for $N > 56$, whereas the HFB solutions indicate prolate–oblate shape coexistence with small energy differences between the two shapes, e.g. less 0.2 MeV for $N = 56$. Comparison to the β_2 values extracted from the data strongly supports the conclusion of prolate shapes for the $N > 60$ Zr nuclei.

The direct comparison between experimentally determined $B(E2; 2_1^+ \rightarrow 0^+_{g.s.})$ values and model predictions provides significant insight to microscopic structure. In particular, the projected shell model (PSM) provides the framework in which the single-particle shell model can be applied to deformed nuclei. The PSM calculations depicted in Fig. 3(a) (dotted line) [38] use deformations from Ref. [47] as input parameters, with the exception of ^{104}Zr for which the β_2 value is artificially reduced. The predicted $B(E2; 2_1^+ \rightarrow 0^+_{g.s.})$ values are particularly sensitive to the quadrupole–quadrupole interaction [38], which is derived self-consistently with the β_2 parameter. Therefore, experimentally derived $B(E2; 2_1^+ \rightarrow 0^+_{g.s.})$ values are a valuable constraint to impose on the model.

The solid line in Fig. 3(a) shows the $B(E2; 2_1^+ \rightarrow 0^+_{g.s.})$ values calculated using the interacting boson model (IBM-1) [39] and a set of global parameters. Whilst the results do show a maximum

$B(\mathrm{E2}; 2_1^+ \rightarrow 0_{g.s.}^+)$ value at $N = 64$, the maximum is significantly lower than that observed. This difference could be due to fact that the parameters of the Hamiltonian were obtained through fitting to energy levels and B(E2) values of the triaxially deformed nuclei Mo, Pd and Ru nuclei [49,50,22,51] in addition to the well deformed $N \geq 60$ Zr nuclei. Since the energy levels and B(E2) values of triaxial Mo and Ru isotopes are well reproduced [39], the deviation of the calculations to the observations may be attributed to the IBM-1 Hamiltonian not reflecting the axial symmetry of the zirconium nuclei for $N > 60$.

In summary, we have reported on lifetime measurements of 2_1^+ states in ^{104,106}Zr, which show that ^{104}Zr is the most deformed of the neutron-rich Zr isotopes. In addition, comparison of the magnitude of the extracted deformation with the results of model calculations [47,48] indicate that these nuclei are prolate deformed. Moreover, we have demonstrated that the technique of lifetime measurements following the β-decay of RI beams is a feasible method of extracting spectroscopic information at the contemporary limits of experimentally accessible nuclei. Such techniques can be further exploited at the RIBF, and also at future projects such as FAIR [52,53].

Acknowledgements

We would like to express our gratitude to the RIKEN Nishina Center accelerator department for providing a stable and high intensity ^{238}U primary beam. F.B. is grateful to C.R. Nita for invaluable discussions on fast-timing measurements using $LaBr_3$(Ce) detectors. This work was supported by JSPS KAKENHI Grants Nos. 26800117 and 25247045. UK authors were supported by STFC Grant Nos. ST/J000132/1, ST/J000051/1 and ST/K502431/1. P.H.R. acknowledges support from the UK National Measurement Office (NMO). P.-A.S. was financed by JSPS Grant No. 23 01752 and the RIKEN Foreign Postdoctoral Researcher Program. V.W. was supported by DOE Grant No. DE-FG02-91ER-40609. J.T. was financed by Spanish Ministerio de Ciencia e Innovación under Contracts No. FPA2009-13377-C02 and No. FPA2011-29854-C04. We acknowledge the EUROBALL Owners Committee for the loan of germanium detectors and the PreSpec Collaboration for the readout electronics of the cluster detectors.

References

[1] O. Haxel, J.H.D. Jensen, H.E. Suess, On the "magic numbers" in nuclear structure, Phys. Rev. 75 (1949) 1766.
[2] M.G. Mayer, On closed shells in nuclei. II, Phys. Rev. 75 (1949) 1969.
[3] W. Nazarewicz, Microscopic origin of nuclear deformations, Nucl. Phys. A 574 (1994) 27.
[4] K. Kaneko, M. Hasegawa, T. Mizusaki, Y. Sun, Magicity and occurrence of a band with enhanced $B(E2)$ in neutron-rich nuclei ^{68}Ni and ^{90}Zr, Phys. Rev. C 74 (2006) 024321.
[5] P.E. Garrett, W. Younes, J.A. Becker, L.A. Bernstein, E.M. Baum, D.P. DiPrete, R.A. Gatenby, E.L. Johnson, C.A. McGrath, S.W. Yates, M. Devlin, N. Fotiades, R.O. Nelson, B.A. Brown, Nuclear structure of the closed subshell nucleus ^{90}Zr studied with the $(n, n'\gamma)$ reaction, Phys. Rev. C 68 (2003) 024312.
[6] V. Werner, et al., Evidence for the microscopic formation of mixed-symmetry states from magnetic moment measurements, Phys. Rev. C 78 (2008) 031301.
[7] A. Chakraborty, et al., Collective structure in ^{94}Zr and subshell effects in shape coexistence, Phys. Rev. Lett. 110 (2013) 022504.
[8] I. Boboshin, V. Varlamov, B. Ishkhanov, E. Romanovsky, New double-magic nucleus ^{96}Zr and conditions for existence of new magic nuclei, Phys. At. Nucl. 70 (2007) 1363.
[9] S. Rinta-Antila, S. Kopecky, V.S. Kolhinen, J. Hakala, J. Huikari, A. Jokinen, A. Nieminen, J. Äystö, J. Szerypo, Direct mass measurements of neutron-rich zirconium isotopes up to ^{104}Zr, Phys. Rev. C 70 (2004) 011301.
[10] J.E. García-Ramos, K. Heyde, R. Fossion, V. Hellemans, S. De Baerdemacker, A theoretical description of energy spectra and two-neutron separation energies for neutron-rich zirconium isotopes, Eur. Phys. J. A 26 (2005) 221.
[11] S. Anghel, G. Cata-Danil, N.V. Zamfir, Structure features revealed from the two neutron separation energies, Rom. J. Phys. 54 (2009) 301.
[12] E. Cheifetz, R.C. Jared, S.G. Thompson, J.B. Wilhelmy, Experimental information concerning deformation of neutron rich nuclei in the A ∼ 100 region, Phys. Rev. Lett. 25 (1970) 38.
[13] T. Sumikama, et al., Structural evolution in the neutron-rich nuclei ^{106}Zr and ^{108}Zr, Phys. Rev. Lett. 106 (2011) 202501.
[14] S. Michiaki, A. Akito, Shape transition of nuclei with mass around A = 100, Nucl. Phys. A 515 (1990) 77.
[15] P. Federman, S. Pittel, Unified shell-model description of nuclear deformation, Phys. Rev. C 20 (1979) 820.
[16] W. Urban, J. Pinston, T. Rzaca-Urban, A. Złomaniec, G. Simpson, J. Durell, W. Phillips, A.G. Smith, B. Varley, I. Ahmad, N. Schulz, First observation of the $\nu 9/2[404]$ orbital in the A ∼ 100 mass region, Eur. Phys. J. A 16 (2003) 11.
[17] W. Urban, J. Pinston, J. Genevey, T. Rzaca-Urban, A. Złomaniec, G.S. Simpson, J. Durell, W. Phillips, A.G. Smith, B. Varley, I. Ahmad, N. Schulz, The $\nu 9/2[404]$ orbital and the deformation in the A ∼ 100 region, Eur. Phys. J. A 22 (2004) 241.
[18] W. Nazarewicz, in: International Conference on Contemporary Topics in Nuclear Structure Physics, World Scientific, 1988, pp. 467–486.
[19] A.G. Smith, et al., The influence of $\nu h 11/2$ occupancy on the magnetic moments of collective 2_1^+ states in A ∼ 100 fission fragments, Phys. Lett. B 591 (2004) 55.
[20] P. Campbell, H.L. Thayer, J. Billowes, P. Dendooven, K.T. Flanagan, D.H. Forest, J.A.R. Griffith, J. Huikari, A. Jokinen, R. Moore, A. Nieminen, G. Tungate, S. Zemlyanoi, J. Äystö, Laser spectroscopy of cooled zirconium fission fragments, Phys. Rev. Lett. 89 (2002) 082501.
[21] Y. Luo, et al., Shape transitions and triaxiality in neutron-rich odd-mass Y and Nb isotopes, Eur. Phys. J. A (Suppl.) 25 (2005) 469.
[22] H. Watanabe, et al., Development of axial asymmetry in the neutron-rich nucleus ^{110}Mo, Phys. Lett. B 704 (2011) 270.
[23] A.M. Bruce, et al., Shape coexistence and isomeric states in neutron-rich ^{112}Tc and ^{113}Tc, Phys. Rev. C 82 (2010) 044312.
[24] P.-A. Söderström, et al., Shape evolution in ^{116,118}Ru: triaxiality and transition between the O(6) and U(5) dynamical symmetries, Phys. Rev. C 88 (2013) 024301.
[25] H. Mach, F. Wohn, G. Molnár, K. Sistemich, J.C. Hill, M. Moszyński, R. Gill, W. Krips, D. Brenner, Retardation of $B(E2; 0_1^+ \rightarrow 2_1^+)$ rates in $^{90-96}$Sr and strong subshell closure effects in the A ∼ 100 region, Nucl. Phys. A 523 (1991) 197.
[26] M. Bender, K. Bennaceur, T. Duguet, P.H. Heenen, T. Lesinski, J. Meyer, Tensor part of the Skyrme energy density functional. II. Deformation properties of magic and semi-magic nuclei, Phys. Rev. C 80 (2009) 064302.
[27] T. Kubo, D. Kameda, H. Suzuki, N. Fukuda, H. Takeda, Y. Yanagisawa, M. Ohtake, K. Kusaka, K. Yoshida, N. Inabe, T. Ohnishi, A. Yoshida, K. Tanaka, Y. Mizoi, BigRIPS separator and ZeroDegree spectrometer at RIKEN RI Beam Factory, Prog. Theor. Exp. Phys. 2012 (2012) 03C003.
[28] N. Fukuda, T. Kubo, T. Ohnishi, N. Inabe, H. Takeda, D. Kameda, H. Suzuki, Identification and separation of radioactive isotope beams by the BigRIPS separator at the RIKEN RI Beam Factory, Nucl. Instrum. Methods Phys. Res., Sect. B, Beam Interact. Mater. Atoms 317 (2013) 323.
[29] T. Sumikama, et al., Structure of neutron-rich Zr and Mo isotopes, RIKEN Accel. Prog. Rep. 47 (2014) 9.
[30] S. Nishimura, Beta-gamma spectroscopy at RIBF, Prog. Theor. Exp. Phys. 2012 (2012) 03C006.
[31] Z. Patel, et al., Commissioning of a $LaBr_3$(Ce) array with EURICA at RIBF, RIKEN Accel. Prog. Rep. 47 (2014) 13.
[32] P.-A. Söderström, et al., Installation and commissioning of EURICA – Euroball-RIKEN Cluster Array, Nucl. Instrum. Methods Phys. Res., Sect. B, Beam Interact. Mater. Atoms 317 (2013) 649.
[33] A.G. Smith, et al., Lifetimes of yrast rotational states of the fission fragments ^{100}Zr and ^{104}Mo measured using a differential plunger, J. Phys. G 28 (2002) 2307.
[34] H. Ohm, M. Liang, G. Molnár, K. Sistemich, The collectivity in the yrast band of ^{100}Zr: the half-life of the 4_1^+ state, Z. Phys. A 334 (1989) 519.
[35] C. Hutter, et al., $B(E2)$ values and the search for the critical point symmetry X(5) in ^{104}Mo and ^{106}Mo, Phys. Rev. C 67 (2003) 054315.
[36] H. Hua, C.Y. Wu, D. Cline, A.B. Hayes, R. Teng, R.M. Clark, P. Fallon, A. Goergen, A.O. Macchiavelli, K. Vetter, Triaxiality and the aligned h_{112} neutron orbitals in neutron-rich Zr and Mo isotopes, Phys. Rev. C 69 (2004) 014317.
[37] J.K. Hwang, A.V. Ramayya, J.H. Hamilton, Y.X. Luo, A.V. Daniel, G.M. Ter-Akopian, J.D. Cole, S.J. Zhu, Half-life measurements of several states in ^{95,97}Sr, ^{97,100,104}Zr, ^{106}Mo, and ^{148}Ce, Phys. Rev. C 73 (2006) 044316.
[38] Y.-X. Liu, Y. Sun, X.-H. Zhou, Y.-H. Zhang, S.-Y. Yu, Y.-C. Yang, H. Jin, A systematical study of neutron-rich Zr isotopes by the projected shell model, Nucl. Phys. A 858 (2011) 11.
[39] M. Böyükata, P.V. Isacker, İ. Uluer, Description of nuclei in the A ∼ 100 mass region with the interacting boson model, J. Phys. G 37 (2010) 105102.
[40] D. Abriola, A. Sonzogni, Nuclear data sheets for A = 96, Nucl. Data Sheets 109 (2008) 2501.
[41] B. Singh, Z. Hu, Nuclear data sheets for A = 98, Nucl. Data Sheets 98 (2003) 335.

[42] B. Singh, Nuclear data sheets for A = 100, Nucl. Data Sheets 109 (2008) 297.
[43] D.D. Frenne, Nuclear data sheets for A = 102, Nucl. Data Sheets 110 (2009) 1745.
[44] J. Blachot, Nuclear data sheets for A = 104, Nucl. Data Sheets 108 (2007) 2035.
[45] S. Raman, C.W. Nestor Jr., P. Tikkanen, Transition probability from the ground to the first-excited 2^+ state of even–even nuclides, At. Data Nucl. Data Tables 78 (2001) 1.
[46] K.E.G. Lobner, M. Vetter, V. Honig, Nuclear intrinsic quadrupole moments and deformation parameters, Nucl. Data Tables A 7 (1970) 495.
[47] P. Moller, J. Nix, W. Myers, W. Swiatecki, Nuclear ground-state masses and deformations, At. Data Nucl. Data Tables 59 (1995) 185.
[48] R. Rodríguez-Guzmán, P. Sarriguren, L. Robledo, S. Perez-Martin, Charge radii and structural evolution in Sr, Zr, and Mo isotopes, Phys. Lett. B 691 (2010) 202.
[49] A. Guessous, et al., Prompt γ-ray spectroscopy of the ^{104}Mo and ^{108}Mo fission fragments, Phys. Rev. C 53 (1996) 1191.
[50] A. Guessous, N. Schulz, W.R. Phillips, I. Ahmad, M. Bentaleb, J.L. Durell, M.A. Jones, M. Leddy, E. Lubkiewicz, L.R. Morss, R. Piepenbring, A.G. Smith, W. Urban, B.J. Varley, Harmonic two-phonon γ-vibrational state in neutron-rich ^{106}Mo, Phys. Rev. Lett. 75 (1995) 2280.
[51] S. Lalkovski, et al., Two-quasiparticle and collective excitations in transitional ^{108,110}Pd nuclei, Eur. Phys. J. A 18 (2003) 589.
[52] O.J. Roberts, A.M. Bruce, P.H. Regan, Z. Podolyák, C.M. Townsley, J.F. Smith, K.F. Mulholland, A. Smith, A $LaBr_3$: Ce fast-timing array for DESPEC at FAIR, Nucl. Instrum. Methods Phys. Res., Sect. A, Accel. Spectrom. Detect. Assoc. Equip. 748 (2014) 91.
[53] P. Regan, From RISING to the DESPEC fast-timing project within NUSTAR at FAIR: sub-nanosecond nuclear timing spectroscopy with $LaBr_3$ scintillators, Appl. Radiat. Isot. 70 (2012) 1125.